Available online at www.sciencedirect.com

SciVerse ScienceDirect

Procedia CIRP 1 (2012) 546 – 551

www.elsevier.com/locate/procedia

5th CIRP Conference on High Performance Cutting 2012

In-Process Deformation Measurement of thin-walled Workpieces

J. Loehe[a]*, M. F. Zaeh[a], O. Roesch[a]

[a]*Institute for Machine Tools and Industrial Management - TU Muenchen, Boltzmannstr. 15, Garching 85748, Germany*
*Corresponding author. Tel.: +49(0) 89/289 15512; fax: +49(0) 89/289 15555; E-mail address: Johannes.Loehe@iwb.tum.de.

Abstract

During the finish milling process of thin-walled workpieces, deformations occur due to the mechanical and thermal influences. The measuring method outlined in this publication allows an accurate assignment of these deformations to their respective cause in size and form, due to the high temporal and spatial resolution of the used optical measurement system. Furthermore, dividing the displacement into its mechanical and thermal proportion allows a fully decoupled validation of process models. Especially the simulation results of thermal models, which are mainly validated by measured temperature fields, can be further ensured.

Keywords: Cutting; Deformation; In-process measurement; Laser scanning; Milling

1. Introduction

Short production cycles and a high level of cost-efficiency are some of the main aims within the design of production technologies. The advancements of cutting materials, drive and control systems as well as the improvements regarding the structural behaviour of machine tools ensure steadily increasing reliability and reproducibility of metal cutting operations. Deformations, caused by thermal and mechanical influences of the process, can occur and may substantially affect the machining results of complex, thin-walled workpieces. Within the framework of the research project "Modelling, Simulation, and Compensation of Thermal Effects for Complex Machining Processes" (SPP 1480) funded by the DFG (German Research Foundation), several machining operations shall be examined with focus on the resulting deviation in terms of shape and dimension. The Institute for Machine Tools and Industrial Management (iwb) of the Technische Universitaet Muenchen (TUM) explicitly studies in the SPP 1480 the helical end milling process. The project aims to couple known analytical approaches, which describe the forces and the heat flux out of the process with a discrete structural model of the workpiece in order to predict the occurring deformations quickly and reliably. To verify the analytical submodels of the force and the heat flux, measurements of the force and the temperature are essential. Measuring the displacements of the workpiece during the milling process in addition enables further verification of the analytical models as well as the validation of the resulting displacements, calculated by the numerical discrete model of the workpiece.

1.1. Thermomechanically caused deformation during the milling of thin-walled workpieces

Due to the finishing process of thin-walled workpiece structures, such as aircraft components and motor vehicle engines, deformations occur. These deflections are caused by mechanical and thermal process influences and can be both of elastic and plastic nature. In their approaches [1] and [2] already describe the deformation behaviour of such thin-walled workpiece structures during the milling in analytical form. [3], [4], [5], [6] and [7] examine this with numerical models.

However, with the process parameters examined in the context of this work, a full spring-back of the thin-walled structure occurs (see section 2.2). For this reason, in the following only elastic deformations must be treated. To capture elastic displacements, it is absolutely necessary to measure during the machining process. The approaches of [2], [4], [5] and [8] describe such in-process measurement methods. Mostly, inductive ([2],

 http://dx.doi.org/10.1016/j.procir.2012.04.097

[4] and [8]) or tactile ([5]) methods are used for this purpose. With inductive methods, only deformations of large areas, but not highly resolved points are measurable, which is one of the main disadvantages of this technique. In addition the rotating milling tool behind the thin-walled structure might affect the impedance negatively. Besides this, a capacitive sensor cannot distinguish a tilt from a pure translation of the measured area. Tactile gauges can affect the dynamic deformation behaviour of thin-walled workpiece structures negatively. Therefore, this research describes an alternative method that allows the precise determination of the deformation using a non-contact optical measurement system. The measuring equipment used for this approach is a 3D-Scanning-Laser-Doppler-Vibrometer (LDV) of the company Polytec. Its functionality is described in the following section.

1.2. Functional Principle of the LDV

The system, shown in Figure 1, consists of three scan heads, which are mounted at a tripod. Every scan head contains a laser interferometer, a video camera and a dual-axis scanning-mirror to deflect the laser beam horizontally and vertically in a range of $\pm 20°$. A laser interferometer is a very precise (resolution of the measuring system from the data sheet: $2.26\ \frac{\mu m}{s}$) optical transducer used to determine the velocity of a point by sensing the frequency shift of the back-scattered light from a moving surface. After a calibration of the system, it is possible to define the measuring points directly on the video image of the test object. Subsequently, the coordinates of every point are measured by a geometry scan unit, which is attached to the top scan head.

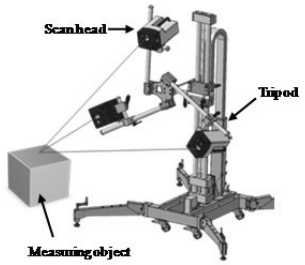

Fig. 1. Setup of the measurement system

During the measurement, the three laser beams are directed to one specific point while every scan head determines the beam-directional velocity of this point. The software calculates the three-dimensional vibration vector by trigonometric transformation. The results can be evaluated in the time and frequency domain and be numerically integrated to determine the displacement of the measurement points [9].

2. Measuring elastic deformations during the milling process

As already mentioned in section 1.1, it is only necessary to acquire the elastic deformation. Within a topology determination following the milling process, elastic deflections can be approximated roughly, but a differentiation between mechanically and thermally caused deformations is not possible. Therefore, an in-process method and its possibilities are presented subsequently.

2.1. Experimental setup

The visual accessibility of the workpiece is mandatory for the deformation measurement with the LDV. For that reason, milling experiments were conducted on a portal milling machine with a very open structure (Virtumat, Fig. 2). This machine allows the continuous acquisition of the measuring point.

Fig. 2. Portal milling machine

It must also be avoided that chip flow disturbs the measuring beam, as this would cause an overrange of the decoder and make the signal unusable. Therefore, a sheet is mounted with a small gap to the workpiece, so that any influence on the dynamic behaviour could be ruled out. Besides these relevant conditions for the method of measurement, the workpiece is clamped over its whole length inside a hydraulic vice in order to exclude additional influence from cutting forces in cantilevered border regions.

The milling experiments were conducted with a Tantal coated carbide end milling cutter with three teeth (Type 434) of the company HAM Tools GmbH (Fig. 3).

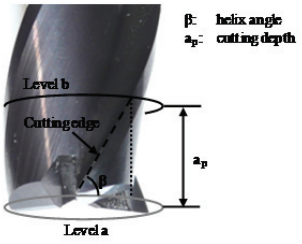

Fig. 3. Experimental milling tool (Co. HAM Tools GmbH - Type 434; diameter $d = 16$ mm; helix angle $\beta = 30°$; chamfer $b = 0.1$ mm)

Usually, a small cutting width (a_e) is used for finishing processes. Therefore, the parameter window implies values of $0.5\,\text{mm} \leq a_e \leq 2\,\text{mm}$ and a simultaneous variation of the cutting depth between 4 mm and 10 mm. Within these parameters, the process remains stable. Considering effects of chatter is therefore not necessary. The schematic experimental procedure is outlined in Fig. 4. The initially 10 mm thick workpiece gets reduced in thickness by multiple radial feed with cutting width a_e, so that the remaining bar gets thinner and thinner. Further dimensions can be found in the sketch below (Fig. 4). These are mainly the parameters influencing the deformation.

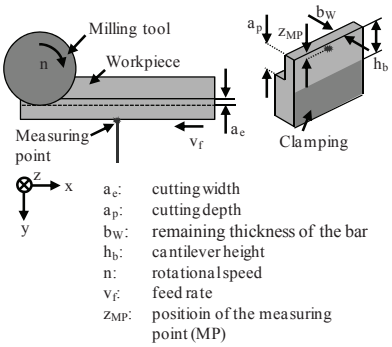

Fig. 4. Schematic experimental setup

The laser spot of the LDV is placed in x-direction centrally and 2 mm below the upper edge in z-direction. For this application, the LDV operates at a sampling rate of 12.8 kHz, which is sufficient to resolve the deflection (tooth passing frequency: 75 Hz to 150 Hz).

2.2. Interpretation of the measurement signal

Considering the measurement signal in y-direction versus the time of the machining process (see Fig. 5), the static and dynamic deformation components can be seen directly. Their cause is derived from simple geometric considerations within this chapter.

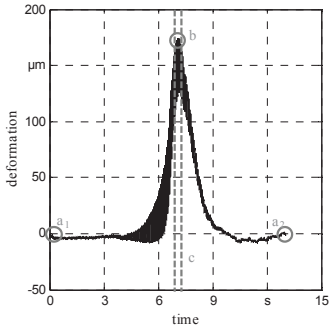

Fig. 5. Measured deformation ($a_p = 10$ mm; $a_e = 1$ mm; $n = 2000\,\frac{1}{\text{min}}$; $f_z = 0.1$ mm; $b_W = 0.5$ mm; a_1: first cut; a_2: last cut; b: maximum of deformation; c: representative area)

An important conclusion can be drawn by considering the marked areas a_1 and a_2 inside Fig. 5. After the withdrawal of the milling tool in a_2, the initial value a_1 is reached again. This aspect occurs for the whole range of examined parameters. In consequence, plastic deformation of the remaining material (bar) can be excluded for those parameters.

Furthermore, the maximum of deformation (Fig. 5, marking b) is still striking. As expected, the maximum deflection is consistent with the time the cutting edge enters the material directly located in position with the stationary measuring point.

For a detailed geometric consideration, area c (Fig. 5) is enlarged in Fig. 6. This diagram includes explicitly the three single cutting edge contacts of the milling tool. These are very finely resolved due to the high temporal measuring resolution of 12.8 kHz.

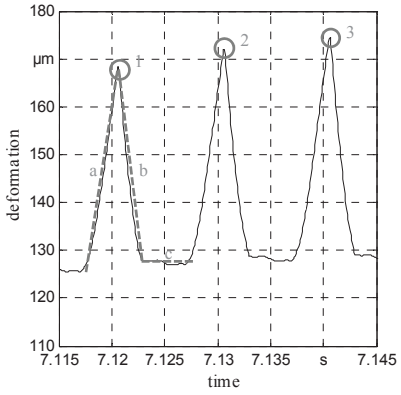

Fig. 6. Representative area c from Fig. 5 (a: rising flank; b: falling flank; c: plateau; 1, 2, 3: maximum elastically deformation by each of the three teeth)

The different height of the deformation peaks (Fig. 6, marking 1, 2, 3) is in this case (new, wear-free milling tool) based on the varying edge length of each tool tooth. Future studies should also pay attention to the wear of the cutting edge. However, that plays only a minor role for the envisaged use of the procedure as a validation method. The characteristic of the dynamic part of the signal is quite more important and will be interpreted within the following section of this chapter.

The rising of flank a (Fig. 6) can be explained by observing the cutting edge, which enters the material at the beginning and then gets more and more in contact, caused by the pitch angle of the milling tool (Fig. 7, contact a). As soon as the cutting edge exits the workpiece (Fig. 7, contact b) and thus no longer covers the entire cutting width a_e, the deformation falls off again (Fig. 6, marking b). If the milling tool turns further, a short period with no physical contact between the cutter and the workpiece remains (Fig. 7, contact c). This area is characterized by the plateau in the measuring signal

(Fig. 6, marking c). As previously mentioned, there is no contact on the plateau c and in consequence no elastic deformation can be caused by the milling tool there. Recognizing that no plastic deformations are induced by the process, only thermal effects can affect the displacements in c. This preliminary conclusion allows breaking down the measured signal into a mechanical and a thermal part. Therefore, the plateaus (Fig. 6, marking c), which represent the thermally induced deformations are detected by a windowed (width of the tooth path frequency) analysis. The mechanically induced deformations are determined by deducting the detected values from the measured signal.

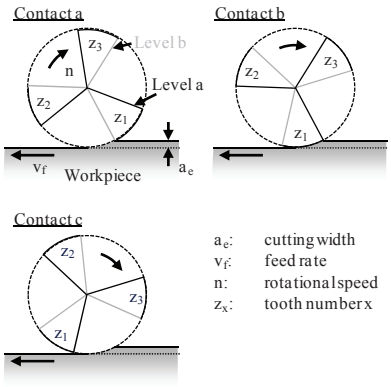

Fig. 7. Schematic contact between the milling tool and the workpiece

In order to reinforce the approach, a comparison of the extracted thermal displacement signal and a scaled picture of the temperature field on the back of the part is shown in Fig. 8.

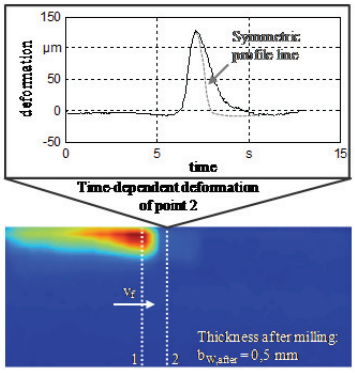

Fig. 8. Comparison between the extracted thermal displacement and the temperature field

To explain the relationship between both pictures shown in Fig. 8 and to derive the plausibility of the approach of purely thermally induced deformation, the measuring result is also discussed section by section. Therefore, the deformation of a specific, not moving point 2 on the workpiece is monitored versus the process time (Fig. 8). Point 1 represents the position of the tooth entering and following the maximum of the temperature induced deformation. This point moves forward with the feed rate v_f.

- Point 1 on the left of point 2:
  Due to the stiffness of the workpiece, the deflection of point 1 causes a smaller deformation at point 2. The closer the milling tooth impact (1) gets to point 2, the more it will be deformed.
- Point 1 matching with point 2:
  The temperature field induces the deformation of point 2 directly and deforms it maximally (Peak of Fig. 8)
- Point 1 on the right of point 2:
  As explained in the first bullet, point 2 gets deformed due to the compliance of the workpiece. This would lead to the symmetric profile line of Fig. 8. In addition, the trailing temperature field induces a thermal expansion and in consequence further deformation of point 2. This leads to the characteristic unsymmetrical deformation curve shown in Fig. 8 and confirms the assumption.

Based on the results, it becomes possible to separate thermal and mechanical deformations. Resulting benefits are presented within the next chapter.

2.3. Discussion of the in-process measuring results

The following subsection exclusively discusses the mechanically influenced deformations in dependence of several process parameters. The remaining thickness on the bar, which is shown in Fig. 9, should be noted in this context.

This example includes the measured values of 36 milling operations in order to get a fine gradation over the remaining bar thickness. It becomes apparent that a strong dependency exists between the deformation and the remaining thickness. This is a reasonable result, because the stiffness of the part shrinks with the decreasing thickness of the workpiece. Thus, deformations caused by forces become larger.

Further influencing factors on the mechanically induced deformation of the workpiece are the clamping conditions (unsupported height h_B) as well as the milling parameters (cutting depth a_p, cutting width a_e, rotational speed n, feed per tooth f_z).

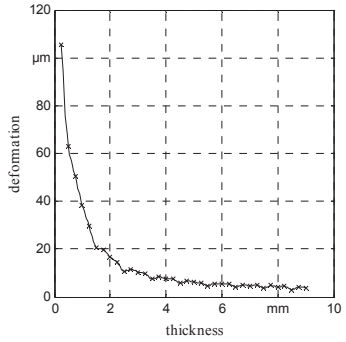

Fig. 9. Mechanically induced deformation in dependence of the remaining thickness of the workpiece ($a_p = 10$ mm; $a_e = 1$ mm; $n = 2000\,\frac{1}{\text{min}}$; $f_z = 0.1$ mm)

The wear of the milling tool also affects the deformation, but cannot be evaluated on the basis of the experiments conducted so far. Some mechanically induced deformation curves, which differ by a variation of the previously mentioned parameters, are shown in Fig. 10.

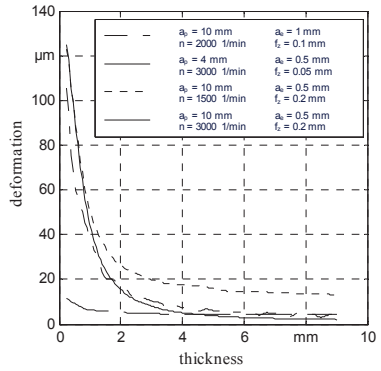

Fig. 10. Mechanically induced deformation in dependence of the remaining thickness of the workpiece and on the variation of other parameters

It follows from Fig. 10 that cutting with low depth a_p leads to a significantly reduced mechanical deformation. Furthermore, differing deformation levels in the range of thicker bars can be seen. These are obviously depending on the rotational speed and the feed per tooth of the milling tool. As the parameters of the shown measurement signals vary, double effects cannot be ruled out. The extension of the experiments will reveal additional relationships between the parameters and the deformation behaviour. This also applies to the parameter dependency of the thermally related displacements. Therefore, the following subsection will not treat the dependency on the clamping conditions and the milling parameters.

The relationship between the remaining bar thickness and the thermally induced deformation should still be considered. Fig. 11 shows this dependency graphically.

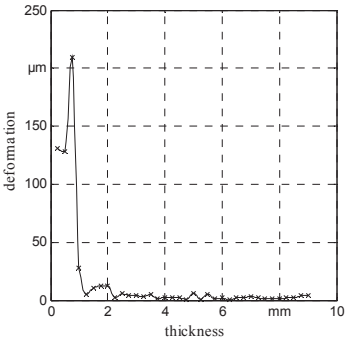

Fig. 11. Thermally induced deformation in dependence on the remaining thickness of the workpiece ($a_p = 10$ mm; $a_e = 1$ mm; $n = 2000\,\frac{1}{\text{min}}$; $f_z = 0.1$ mm)

Not only the sharp increase of the deformation, but also the following drop with a further decrease of the bar thickness is remarkable. This effect can also be observed during laser beam welding of thin-walled sheet metal due to the unilateral heat input.

The resulting temperature field in the shown example (Fig. 12) remains nearly the same, only influenced by a minimally modified heat dissipation, which is caused by the bar getting thinner. However, the temperatures on the reverse side of the bar are still low at this time. This asymmetrical heat distribution leads to highly different strains of the workpiece material, which ultimately leads to the deflection of the bar (Fig. 12, cross section a).

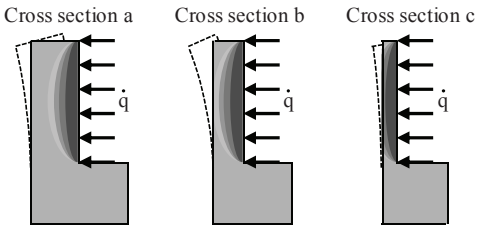

Fig. 12. Principle sketch of temperature field in cross section with different bar thicknesses

With a further reduction of the thickness of the workpiece, its stiffness decreases and the resulting displacement gets higher (Fig. 12, cross section b). At a specific bar width, the smaller temperature gradient of the bar causes a decrease of the thermally induced deflections. This leads to similar temperatures on both sides of the workpiece and thus to related deformations. As soon as the specific thickness is reached, this effect dominates the decrease of the stiffness and in consequence, the displacements will become smaller.

2.4. Conclusion to the in-process deformation measurement

The effects described within the previous section allow the separate consideration of the mechanically as well as the thermally caused deformations of the workpiece structure. This method represents one more possibility for the validation of process force and heat flux models, which are used to predict the displacements within the framework of SPP 1480.

The heat flux model should be mentioned particularly in this context, which is validated so far by means of temperature measurements on the back side of the bar. However, this temperature field is not a result of a unique heat source, but instead reachable through multiple sources. In combination with the measured thermal deformation, the solution space for shape and size of the heat sources can be concluded to a unequivocal one. This may be explained due to the fact that the deflection of the bar is caused by the temperature fields on both sides of it. As long as the simulated deformation and the temperature field on the back side of the bar match with their particular real values, the simulated temperature field on the processing side must be correct in consequence. Provided that this approach applies for multiple process parameters, it is assumed that the simulated heat source is equal to the real heat input of the process. The effect of the decreasing deformation, which can be derived from the temperature gradient of the bar, can be used as one more validation criterion.

3. Conclusion and Perspectives

Within this paper, three main contents are presented:

- Identification of the deformation causes (plastical-mechanical, elastical-mechanical and elastical-thermal), by measuring those in-process using a high resolution optical system.
- Separating thermally and mechanically induced deformations due to an exclusion of plastically deflections and to the explizit examination of the finishing process.
- Determination of the interdependence of the process parameters and measured deformations

The described deformation measurement was realized for some selected parameters. Extending this approach to the whole parameter spectrum is one of the main aims in the next stage of this project. Furthermore, the same measurements should be realized on other machine tools.

In addition, the separation of mechanically and thermally caused deformations gives an insight, how far each of them can be compensated. It is therefore envisaged to avoid the mechanical part of the displacement by a counter stimulation. The compensation of the thermal part should use the previously described effect of symmetrical temperature distribution. To achieve this, a laser, which is already integrated in a milling machine, should induce the same level of heat on the back side of the bar, as the milling process does. The omittance of the thermal strain on both sides would be the result.

Acknowledgements

We extend our sincerest gratitude to the German Research Foundation (DFG) for the generous support of the work described in this paper.

Furthermore, the authors gratefully acknowledge the support of the TUM Graduate Faculty Center Mechanical Engineering at Technische Universitaet Muenchen, Germany.

References

[1] Budak E., Analytical models for high performance milling. Int. J. of Machine Tools and Manufacture; 2009, vol. 46, pp. 1478–1488.

[2] Ratchev S., Liu S., Huang W., Becker A., A flexible force model for end milling of low-rigidity parts. J. of Materials Processing Technology; 2004, vol. 153-154, pp. 134-138.

[3] Bai W., Zhu X., Finite element simulation and analysis of part deformation induced during milling of thin-walled aerospace monolithic structure parts. IEEE I. Converence on Intelligent Computing and Intelligent Systems; 2010, pp. 440-444.

[4] Rai J. K., Xirouchakis P., Finite element method based machining simulation environment for analyzing part errors induced during milling of thin-walled components. I. J. of Machine Tools and Manufacture; 2008, vol. 48, pp. 629-643.

[5] Tsai J. S., Liao C. L., Finite-element modeling of static surface errors in the peripheral milling of thin-walled workpieces. J. of Materials Processing Technology; 1999, vol. 94, pp. 235-246.

[6] Chen W., Xue J., Tang D., Chen H., Qu S., Deformation prediction and error compensation in multilayer milling processes for thin-walled parts. I. J. of Machine Tools and Manufacture; 2009, vol. 49, pp. 859-864.

[7] Gang L., Study on deformation of titanium thin-walled part in milling process. J. of Materials Processing Technology; 2009, vol. 209, pp. 2788-2793.

[8] Ratchev S., Liu S., Huang W., Becker A., Error prediction and compensation in machining of low-rigidity parts. I. J. of Machine Tools and Manufacture; 2004, vol. 44, pp. 1629-1641.

[9] Polytec Product Catalogue. (2009), PSV-400 Scanning Vibrometer. Available: http://www.polytec.de.